# Derivation of Phase Functions from Multiply Scattered Sunlight Transmitted Through a Hazy Atmosphere

J. A. WEINMAN AND J. T. TWITTY

*Dept. of Meteorology, University of Wisconsin, Madison 53706*

S. R. BROWNING AND B. M. HERMAN

*Dept. of Atmospheric Physics, University of Arizona, Tucson 85701*

(Manuscript received 18 April 1973, in revised form 18 September 1974)

ABSTRACT

The intensity of sunlight multiply scattered in model atmospheres is derived from the equation of radiative transfer by an analytical small-angle approximation. The approximate analytical solutions are compared to rigorous numerical solutions of the same problem. Results obtained from an aerosol-laden model atmosphere are presented. Agreement between the rigorous and the approximate solutions is found to be within a few percent.

The analytical solution to the problem which considers an aerosol-laden atmosphere is then inverted to yield a phase function which describes a single scattering event at small angles. The effect of noisy data on the derived phase function is discussed.

## 1. Introduction

Sunlight is strongly scattered at small angles by aerosols in the atmosphere. This phenomenon is called the aureole. The brightness of the aureole as a function of scattering angle depends mainly on the size distribution of the aerosols in the atmosphere. If the solar zenith angle becomes large or if the atmosphere is very turbid, multiple scattering will become significant. The analysis by numerical methods of sunlight multiply scattered by a turbid atmosphere is a problem which has become more tractable as computers have become more powerful. However, if one seeks to invert measured solar intensity scattered at small angles in order to derive mean size distributions of the aerosols, the problem remains formidable even with currently available computers. The present study will show that it is possible to approximate the scattered intensity transmitted at small almucantar angles by an analytical function, and that this analytical solution to the transfer equation can be inverted to yield a phase function which defines a single scattering event. Twitty[1] (1975) will demonstrate how the phase functions defined at small scattering angles can be inverted to yield the aerosol size distribution.

This study consists of two parts:

1) The transmitted intensity as a function of almucantar angles is derived from an approximate analytical solution to the equation of radiative transfer. The small-angle approximation solutions will be compared to rigorous numerical solutions of the same problem.

2) The phase function will be derived from the multiply scattered intensity. Errors in the measured intensity will be simulated and the resulting uncertainty in the phase function for single scattering will be determined.

[1] Twitty's paper follows this paper.

## Part I: Derivation of Scattered Intensity as a Function of Almucantar Angle

We will employ a Neumann solution to the equation of radiative transfer (see Irvine, 1965) to compute the multiply scattered radiation intensity. The small-angle approximation to the radiative transfer equation is valid as long as $\sin\Psi \approx \Psi$, where $\Psi$ is the scattering angle. This approach was utilized by Weinman (1968) in his analysis of the solar aureole beneath clouds. The strongly forward-scattered diffraction peak in the aerosol phase function and the Rayleigh molecular phase function are approximated by the sum of several Gaussian functions. This renders it feasible to represent the scattered intensity by an analytical function which is rapidly evaluated on a computer.

The solutions found by the approximate analytical method are compared to rigorous numerical solutions of the radiative transfer equation obtained from the model developed by Herman and Browning (1965). The present numerical model is identical to the earlier

TABLE 1a. Parameters employed in the Gaussian approximation to phase function [Eq. (2a)] for an aerosol-laden atmosphere at $\lambda=0.5\ \mu$m: $\alpha$–$\epsilon$ in units of radians$^2$.

| | | | |
|---|---|---|---|
| $A$ | 4.978 | $\alpha$ | 1.477 E-3 |
| $B$ | 2.251 | $\beta$ | 6.392 E-3 |
| $C$ | 0.789 | $\gamma$ | 4.154 E-2 |
| $D$ | 0.420 | $\delta$ | 2.516 E-1 |
| $E$ | 0.148 | $\epsilon$ | 1.128 |

1965 model with the exception that the phase matrix was expanded into a Fourier series in the azimuth angle. This enables all integrations over azimuth to be performed analytically. A special routine is incorporated for angles at and near the direction of the incoming solar radiation in order to obtain the necessary accuracy and detail of the solution for the region of the aureole. The details of this routine will not be described here, but it is estimated that the rigorous numerical solutions presented here for the aureole are accurate to within $\pm 0.5\%$.

## II. Analysis

We will first develop an approximate solution to the transfer equation for transmitted intensities as a function of almucantar angles.

The first step in this analysis is the development approximations to the phase functions which are the sums of Gaussian functions of the scattering angle $\Psi$.

### I2. Phase function approximation

In order to illustrate the method, we will compute the intensity at $\lambda=0.5\ \mu$m emerging from a turbid atmosphere loaded with volcanic dust. The optical depth of the aerosol, $\tau_a=0.500$, is the maximum aerosol optical depth of an atmosphere loaded with volcanic dust cited by Deirmendjian (1971). The optical depth of clear air, $\tau_m=0.145$, is appropriate for $\lambda=0.5\ \mu$m light.

The size distribution of the aerosol is given by

$$\frac{dn}{dr}=n_0 r^{-3.5}\ [\mathrm{cm}^{-3}\ \mu\mathrm{m}^{-1}],\quad 0.02\ \mu\mathrm{m}\leqslant r\leqslant 5.02\ \mu\mathrm{m}. \tag{1}$$

The index of refraction of the material which comprises the aerosols is taken to be $m=1.54$, this index being attributed to silica hazes by Deirmendjian (1969) and it is close to the $m=1.5$ attributed to the stratospheric aerosol by Junge (1963).

Mie theory is employed to derive the phase function $\mathcal{P}_a(\Psi)$ of the aerosols (see Dave, 1968). Because we are mainly interested in forward scattered light, we will neglect polarization effects by averaging the phase function over both directions of polarization to give $\bar{\mathcal{P}}_a(\Psi)$. The scalar phase function for Rayleigh scattering by molecules, $\bar{\mathcal{P}}_m(\Psi)$, has been documented extensively.

The small-angle approximate solution to the radiative transfer equations requires that the phase function should be the sum of Gaussian functions [see Eq. (17)], i.e.,

$$\frac{\hat{\mathcal{P}}_a(\Psi)}{4\pi}=A\exp(-\Psi^2/\alpha)+B\exp(-\Psi^2/\beta)+C\exp(-\Psi^2/\gamma)+D\exp(-\Psi^2/\delta)+E\exp(-\Psi^2/\epsilon)+\cdots, \tag{2a}$$

$$\frac{\hat{\mathcal{P}}_m(\Psi)}{4\pi}=F\exp(-\Psi^2/\zeta)+\cdots. \tag{2b}$$

The small-angle approximation is valid if

$$2\pi\int_0^{\Psi_{\max}}\frac{\hat{\mathcal{P}}_a(\Psi)}{4\pi}\Psi d\Psi\approx 1 \tag{3}$$

at an angle $\Psi_{\max}$, where $\Psi_{\max}\approx\sin\Psi_{\max}$.

The number of terms in the Gaussian series expansion of the phase function must be less than half the number of angles at which the phase function is evaluated. Obviously more terms will give a better approximation to the actual phase functions; however, the terms are not independent so that phase functions inverted from noisy data are best described by a minimum number of terms (see the discussion in Part II of this paper). It appears that if $I$ measured data are available, then the phase function is best approximated by about $I/4$ Gaussian terms. The constants $A$, $B$, $C$, $D$, $E$ and $\alpha$, $\beta$, $\gamma$, $\delta$, $\epsilon$ are derived from a nonlinear least-squares fit which minimizes

$$\sum_{i=1}^{I}\left[\log\left(\frac{\bar{\mathcal{P}}_a(\Psi_i)}{4\pi}\right)-\log\left(\frac{\hat{\mathcal{P}}_a(\Psi_i)}{4\pi}\right)\right]^2=\text{minimum},\qquad I\gg 10, \tag{4a}$$

and

$$\frac{\hat{\mathcal{P}}_m(\Psi)}{4\pi}\approx\frac{3}{8\pi}\exp(-\Psi^2/2). \tag{4b}$$

Table 1a presents the constants that enable Eq. (2a) to best approximate the phase function for scattering from the aerosols characterized by Eq. (1).

Table 1b presents a comparison between the approximate phase function for $\hat{\mathcal{P}}(\Psi)$, and the actual scalar mean phase functions $\bar{\mathcal{P}}(\Psi)$.

The approximate phase function employed in this analysis is

$$\frac{\hat{\mathcal{P}}(\Psi)}{4\pi}=\frac{\tau_a\hat{\mathcal{P}}_a(\Psi)+\tau_m\hat{\mathcal{P}}_m(\Psi)}{4\pi\tau}, \tag{5}$$

where $\tau_a$ and $\tau_m$ are the optical depths of the aerosols and molecules, respectively, and $\tau$ is the total optical depth of the aerosol-laden atmosphere.

TABLE 1b. Comparison of approximate Gaussian and mean phase functions.

| $\Psi$ (deg) | $\frac{\hat{\Phi}_a(\Psi)}{4\pi}$ | $\frac{\bar{\Phi}_a(\Psi)}{4\pi}$ | $\frac{\hat{\Phi}_m(\Psi)}{4\pi}$ | $\frac{\bar{\Phi}_m(\Psi)}{4\pi}$ |
|---|---|---|---|---|
| 0 | 8.586 | 8.556 | 0.119 | 0.119 |
| 1 | 7.546 | 7.563 | 0.119 | 0.119 |
| 2 | 5.373 | 5.395 | 0.119 | 0.119 |
| 3 | 3.545 | 3.531 | 0.119 | 0.119 |
| 5 | 1.923 | 1.923 | 0.119 | 0.119 |
| 7 | 1.310 | 1.317 | 0.118 | 0.118 |
| 10 | 0.914 | 0.898 | 0.118 | 0.118 |
| 15 | 0.610 | 0.642 | 0.115 | 0.115 |
| 20 | 0.433 | 0.426 | 0.112 | 0.112 |
| 25 | 0.330 | 0.336 | 0.109 | 0.109 |
| 30 | 0.258 | 0.259 | 0.104 | 0.104 |
| 35 | 0.201 | 0.200 | 0.099 | 0.100 |
| 40 | 0.156 | 0.156 | 0.094 | 0.095 |
| 45 | 0.122 | 0.121 | 0.088 | 0.090 |
| 50 | 0.096 | 0.096 | 0.082 | 0.084 |
| 60 | 0.061 | 0.061 | 0.069 | 0.075 |
| 70 | 0.040 | 0.040 | 0.057 | 0.067 |

## I3. Radiative transfer calculations

The equation of radiative transfer which defines the scattered intensity $I(\tau,\mu,\phi)$ is

$$\mu\frac{dI(\tau,\mu,\phi)}{d\tau}=-I(\tau,\mu,\phi)+\frac{\bar{\Phi}(\mu,\phi,\mu_0,0)}{4\pi}\exp(-\tau/\mu_0)$$
$$+\frac{1}{4\pi}\int_{-1}^{1}\int_{0}^{2\pi}\bar{\Phi}(\mu,\phi;\mu',\phi')I(\tau,\mu',\phi')d\phi'd\mu'. \quad (6)$$

The optical depth $\tau$ increases in the nadir direction from the upper boundary; the angle between the downward directed intensity and zenith is $\cos^{-1}\mu$ and the azimuth angle is $\phi$. No diffuse intensity is assumed incident on either boundary of the turbid atmosphere. The intensities are normalized with respect to the incoming solar flux.

We will restrict our attention to intensities measured at a zenith angle $\cos^{-1}\mu_0$ and at a variety of azimuth angles $\phi$. Eq. (6) is transformed from a system of coordinates which employs polar and azimuth angles measured with respect to the local zenith to a system of coordinates measured about the axis of propagation of the incoming solar rays (see Fig. 1). The transformed polar angle is $\Psi$ and the transformed azimuth angle is $\Phi$. The original coordinates are related to the transformed coordinates by

$$\left.\begin{aligned}\overset{*}{\tau}&=\tau\mu_0\\ \mu&=\mu_0\cos\Psi+(1-\mu_0^2)^{\frac{1}{2}}\sin\Psi\sin\Phi\\ \sin\phi&=\sin\Psi\cos\Phi/(1-\mu^2)^{\frac{1}{2}}\end{aligned}\right\}. \quad (7)$$

The intensity measured at zenith angles $\cos^{-1}\mu_0$ satisfies

$$\frac{dI(\overset{*}{\tau},\Psi,\Phi)}{d\overset{*}{\tau}}=-I(\overset{*}{\tau},\Psi,\Phi)+\frac{\bar{\Phi}(\Psi)}{4\pi}\exp(-\overset{*}{\tau})$$
$$+\frac{1}{4\pi}\int_0^{\pi}\int_0^{2\pi}\bar{\Phi}(\Psi,0;\Psi',\Phi')$$
$$\times I(\overset{*}{\tau},\Psi',\Phi')\frac{\partial(\mu',\phi')}{\partial(\Psi',\Phi')}d\Phi'd\Psi'. \quad (8)$$

The Jacobian, $\partial(\mu',\phi')/\partial(\Psi',\Phi')$, becomes relatively simple if $\Psi$, $\Psi'$, $\phi$ and $\phi'$ are small and $\mu$ and $\mu'$ are of the order of $\mu_0$. It is straightforward to compute the Jacobian needed to transform the variables of integration, $\partial(\mu',\phi')/\partial(\Psi',\Phi')\approx\Psi'$.

A Neumann solution can be found for Eq. (8):

$$I(\overset{*}{\tau},\Psi)=\sum_{n=1}^{\infty}I_n(\overset{*}{\tau},\Psi), \quad \Psi>0, \quad (9)$$

$$I_n(\overset{*}{\tau},\Psi)=\int_0^{\tau}J_n(\overset{*}{\tau}',\Psi)k(\overset{*}{\tau}-\overset{*}{\tau}')d\overset{*}{\tau}', \quad (10)$$

$$k(\tau)=\begin{cases}\exp(-\tau), & \tau>0\\ 0, & \tau<0\end{cases} \quad (11)$$

The source function consists of terms

$$J_1(\overset{*}{\tau},\Psi)=\frac{F(\Psi,0)}{4\pi}\exp(-\overset{*}{\tau}), \quad (12a)$$

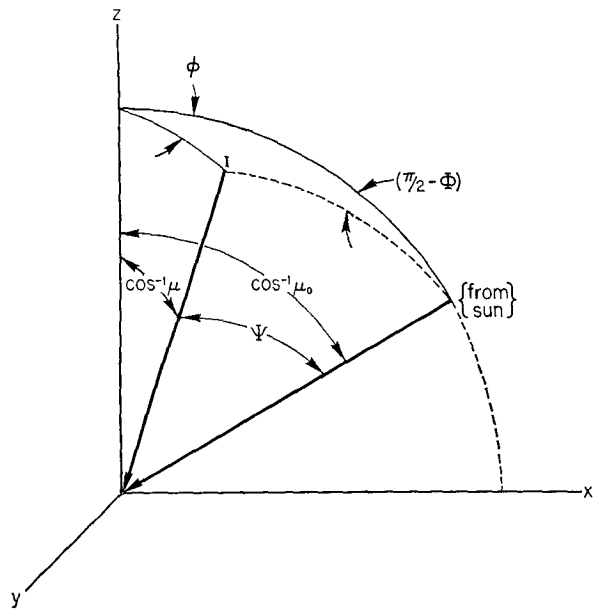


FIG. 1. Schematic view of coordinates.

where

$$F(\Psi_i,\Psi_{i-1})\approx\frac{1}{2\pi}\int_0^{2\pi}\bar{\mathcal{P}}(\Psi_i,\Phi_i;\,\Psi_{i-1},0)d\Phi_i, \quad (12b)$$

$$J_n(\overset{*}{\tau},\Psi)=\Lambda J_{n-1}(\overset{*}{\tau},\Psi). \quad (13a)$$

In addition,

$$\Lambda\{\ \}=\frac{1}{2}\int_0^{\infty}F(\Psi_i,\Psi_{i-1})\Psi_i d\Psi_i \times\int_0^{\overset{*}{\tau}}\{\ \}k(\overset{*}{\tau}-\overset{*}{\tau}')d\overset{*}{\tau}', \quad (13b)$$

$$\vec{\Psi}=\sum_{i=1}^{\infty}\vec{\Psi}_i. \quad (14)$$

The present procedure differs from that described by Irvine (1965) because only small-angle scattering is considered ($\sin\Psi\approx\Psi$, $\cos\Psi\approx 1$) and the upper limit of integration is changed from $\pi$ to $\infty$. No consideration is given to backscattering in the definition of the $\Lambda$ operator because of the small-angle approximation.

The contribution of $n$-fold scattering to the source function is

$$J_n(\overset{*}{\tau},\Psi)=\frac{\overset{*}{\tau}^{n-1}\exp(-\overset{*}{\tau})}{(4\pi)^n(n-1)!}\int_0^{\infty}\cdots\int_0^{\infty}\int_0^{2\pi}\cdots \int_0^{2\pi}\prod_{i=1}^{n}\bar{\mathcal{P}}(\Psi_i,\Phi_i;\,\Psi_{i-1},0)d\Phi_i\Psi_i d\Psi_i. \quad (15)$$

TABLE 2a. Comparison of exact numerical and approximate analytically computed transmitted intensities emerging from an aerosol-laden atmosphere; $\mu_0=\mu=0.966$, $\tau_a=0.5$, $\tau_m=0.145$.

| Almucantar azimuth $\phi$ (deg) | Scattering angle $\Psi$ (deg) | $I(\phi)$ Exact numerical | $I(\phi)$ Analytical approximation | $I(\phi)$ Single scatter | $N(99\%)$ Scattering events |
|---|---|---|---|---|---|
| 0 | 0 | 2.359 E 0 | 2.344 E 0 | 2.288 E 0 | 3 |
| 1 | 0.3 | 2.339 E 0 | 2.324 E 0 | 2.268 E 0 | 3 |
| 2 | 0.5 | 2.282 E 0 | 2.265 E 0 | 2.209 E 0 | 3 |
| 4 | 1.0 | 2.073 E 0 | 2.050 E 0 | 1.995 E 0 | 3 |
| 6 | 1.6 | 1.781 E 0 | 1.756 E 0 | 1.702 E 0 | 3 |
| 8 | 2.1 | 1.470 E 0 | 1.449 E 0 | 1.396 E 0 | 3 |
| 10 | 2.6 | 1.191 E 0 | 1.178 E 0 | 1.126 E 0 | 3 |
| 12 | 3.1 | 9.704 E-1 | 9.639 E-1 | 9.135 E-1 | 3 |
| 14 | 3.6 | 8.112 E-1 | 8.070 E-1 | 7.580 E-1 | 3 |
| 16 | 4.1 | 7.001 E-1 | 6.944 E-1 | 6.467 E-1 | 3 |
| 18 | 4.6 | 6.198 E-1 | 6.116 E-1 | 5.652 E-1 | 3 |
| 20 | 5.2 | 5.574 E-1 | 5.478 E-1 | 5.026 E-1 | 3 |
| 25 | 6.4 | 4.444 E-1 | 4.353 E-1 | 3.926 E-1 | 3 |
| 30 | 7.7 | 3.734 E-1 | 3.642 E-1 | 3.232 E-1 | 4 |
| 35 | 8.9 | 3.239 E-1 | 3.179 E-1 | 2.788 E-1 | 4 |
| 40 | 10.2 | 2.875 E-1 | 2.859 E-1 | 2.482 E-1 | 4 |
| 50 | 12.6 | 2.376 E-1 | 2.399 E-1 | 2.048 E-1 | 4 |
| 60 | 14.9 | 2.044 E-1 | 2.054 E-1 | 1.725 E-1 | 4 |
| 70 | 17.1 | 1.809 E-1 | 1.791 E-1 | 1.480 E-1 | 4 |
| 80 | 19.2 | 1.629 E-1 | 1.594 E-1 | 1.299 E-1 | 4 |
| 90 | 21.1 | 1.487 E-1 | 1.445 E-1 | 1.164 E-1 | 4 |

TABLE 2b. As in Table 2a except for $\mu_0=\mu=0.423$.

| Almucantar azimuth $\phi$ (deg) | Scattering angle $\Psi$ (deg) | $I(\phi)$ Exact numerical | $I(\phi)$ Analytical approximation | $I(\phi)$ Single scatter | $N(99\%)$ Scattering events |
|---|---|---|---|---|---|
| 0 | 0 | 2.380 E 0 | 2.352 E 0 | 2.217 E 0 | 3 |
| 1 | 0.9 | 2.163 E 0 | 2.128 E 0 | 1.994 E 0 | 3 |
| 2 | 1.8 | 1.667 E 0 | 1.633 E 0 | 1.497 E 0 | 4 |
| 3 | 2.7 | 1.187 E 0 | 1.162 E 0 | 1.032 E 0 | 4 |
| 4 | 3.6 | 8.756 E-1 | 8.563 E-1 | 7.318 E-1 | 4 |
| 5 | 4.5 | 7.040 E-1 | 6.818 E-1 | 5.626 E-1 | 4 |
| 6 | 5.4 | 5.948 E-1 | 5.730 E-1 | 4.583 E-1 | 4 |
| 7 | 6.3 | 5.143 E-1 | 4.962 E-1 | 3.856 E-1 | 4 |
| 8 | 7.2 | 4.549 E-1 | 4.408 E-1 | 3.329 E-1 | 5 |
| 9 | 8.2 | 4.094 E-1 | 3.994 E-1 | 2.946 E-1 | 5 |
| 10 | 9.1 | 3.724 E-1 | 3.683 E-1 | 2.663 E-1 | 5 |
| 12 | 10.9 | 3.189 E-1 | 3.234 E-1 | 2.264 E-1 | 5 |
| 14 | 12.7 | 2.828 E-1 | 2.892 E-1 | 1.965 E-1 | 5 |
| 16 | 14.5 | 2.572 E-1 | 2.604 E-1 | 1.717 E-1 | 5 |
| 18 | 16.3 | 2.375 E-1 | 2.360 E-1 | 1.510 E-1 | 5 |
| 20 | 18.1 | 2.201 E-1 | 2.156 E-1 | 1.341 E-1 | 5 |
| 25 | 22.6 | 1.806 E-1 | 1.779 E-1 | 1.041 E-1 | 5 |
| 30 | 27.1 | 1.525 E-1 | 1.512 E-1 | 8.426 E-2 | 5 |
| 35 | 31.6 | 1.344 E-1 | 1.297 E-1 | 6.890 E-2 | 5 |
| 40 | 36.1 | 1.159 E-1 | 1.113 E-1 | 5.625 E-2 | 5 |
| 45 | 40.6 | 1.004 E-1 | 9.578 E-2 | 4.594 E-2 | 5 |

The Hankel transform of a folded integral such as the one in Eq. (15) is the product of the transforms of the constituents (see Sneddon, 1972). The transform $\tilde{J}_n(\overset{*}{\tau},\xi)$ of Eq. (15) is

$$\tilde{J}_n(\overset{*}{\tau},\xi)=\frac{\overset{*}{\tau}^{n-1}\exp(-\overset{*}{\tau})}{(4\pi)^n(n-1)!}\left[2\pi\int_0^{\infty}J_0(\xi\Psi)\bar{\mathcal{P}}(\Psi)\Psi d\Psi\right]^n, \quad (16)$$

where $J_0(\xi\Psi)$ is a zero-order Bessel function. The integral in Eq. (16) has an analytical solution when $\bar{\mathcal{P}}(\Psi)$ is approximated by the sum of Gaussian functions.

The Gaussian approximation $\hat{\mathcal{P}}(\Psi)$ given in Eqs. (2a), (2b) and (5) may therefore be introduced into Eq. (16).

The inverse Hankel transform is then applied to $\tilde{J}_n(\overset{*}{\tau},\xi)$; inserting the result of the inverse transform into Eqs. (9) and (10) yields the intensity:

$$I(\overset{*}{\tau},\Psi)=\sum_{n=1}^{N}\frac{\overset{*}{\tau}^n e^{-\overset{*}{\tau}}}{4^n}\sum_{m=0}^{n}\sum_{l=0}^{m}\sum_{k=0}^{l}\sum_{j=0}^{k}\sum_{i=0}^{j}\frac{\exp(-\Psi^2/\chi)}{\chi} \times\frac{(\tilde{A}\alpha)^{n-m}(\tilde{B}\beta)^{m-l}(\tilde{C}\gamma)^{l-k}(\tilde{D}\delta)^{k-j}(\tilde{E}\epsilon)^{j-i}(\tilde{F}\zeta)^i}{(n-m)!(m-l)!(l-k)!(k-j)!(j-i)!i!}, \quad (17)$$

where

$$\left.\begin{aligned}\chi&=[(n-m)\alpha+(m-l)\beta+(l-k)\gamma\\&\qquad+(k-j)\delta+(j-i)\epsilon+i\zeta]\\ \tilde{A}&=4\pi A\tau_a/(\tau_a+\tau_m),\quad \tilde{B}=4\pi B\tau_a/(\tau_a+\tau_m)\ldots,\\&\qquad\tilde{F}=4\pi F\tau_m/(\tau_m+\tau_a)\end{aligned}\right\}.$$

This intensity can readily be transformed back to a system of coordinates employing zenith and azimuth angles if the transformations introduced in Eq. (7) are recalled.

### I4. Results

We apply Eq. (17) to an atmosphere characterized by $\tau_m=0.145$, $\tau_a=0.5$, and a phase function which is represented by the data in Table 1. Intensities scattered at $\mu=\mu_0=\cos 15°$ and $\cos 65°$ are presented as a function of almucantar azimuth angle in Tables 2a and 2b, respectively.[2] The results obtained from Eq. (17) are compared with the rigorous numerical solution of Eq. (6). Tables 2a and 2b also show the contribution of the single scattering to the total scattered intensity, the number of scattering events which contribute to more than 99% of the scattered intensity, and the scattering angle, $\Psi=\Psi(\mu_0,\phi)$.

It is evident from Tables 2 that the analytical solution to the radiative transfer equation agrees with the rigorous solution within a few percent. The analytical solution tends to underestimate the scattered intensity because the approximate phase function is less than the actual phase function at large angles. It thus appears that large-angle scattering, which we have underestimated, contributes slightly to the aureole in the cases which we have considered.

It is somewhat gratifying to note that the small-angle approximation works as well as it does when $\Psi>25°$. This may be caused by $\Psi>\sin\Psi$ and $\hat{\mathcal{P}}_a(\Psi)<\bar{\mathcal{P}}_a(\Psi)$ compensating each other at large scattering angles.

Attempts to apply the approximate solution [Eq. (17)] to a pure Rayleigh atmosphere grossly underestimate the scattered intensity. This is caused by the failure of the Rayleigh phase function approximation to satisfy the conditions presented in Eqs. (3) and (4a). The approximate solution works well in the turbid atmosphere considered in the present model because the Rayleigh contribution to Eq. (5) is relatively modest.

## Part II: Derivation of Phase Functions from Intensities Multiply Scattered at Small Angles

Having shown that Eq. (17) is a satisfactory approximation to derive intensities which are multiply scattered at small angles, we now show that it is feasible to invert simulated observations to yield the phase function for a single-scattering event.

We will confine our attention to the previous case for which multiple scattering is most significant, i.e., $\mu_0=0.423$ which is presented in Table 2b. It will be assumed that the optical thickness of the atmosphere can be determined from the measured extinction of the direct solar flux. An optimizing program based on Marquardt's (1963) algorithm is then applied to Eq. (17) to derive the parameters employed in the Gaussian approximation given by Eq. (2a).

The following cases will be considered:

1) A simulated noiseless aureole measured at 20 azimuth angles. (Twenty angles are regarded as a reasonable number of measurements with adequate redundancy.)

2) A simulated noiseless aureole measured at 8 azimuth angles (Eight angles are regarded as the minimum number of measurements which can yield any useful representation of the phase function.)

3) Simulated aureoles with 3% random noise measured at 20 azimuth angles.

4) Simulated aureoles with 10% random noise measured at 20 azimuth angles.

5) Simulated aureoles with 10% random noise measured at 8 azimuth angles.

If 20 simulated noise-free measurements are available, Table 3 shows that it is possible to reconstruct a phase function characterized by eight independent parameters, i.e., $[\hat{\mathcal{P}}_a^{(8)}(\Psi)]/4\pi$ falls within 0.03% of the actual mean phase function $[\bar{\mathcal{P}}_a(\Psi)]/4\pi$. The departure is

TABLE 3a. Comparison between the original phase function and Gaussian approximations derived from noiseless auerole data.

| $\Psi$ (deg) | $\frac{\bar{\mathcal{P}}_a(\Psi)}{4\pi}$ | $\frac{\hat{\mathcal{P}}_a^{(8)}(\Psi)}{4\pi}$ | $\frac{\hat{\mathcal{P}}_a^{(4)}(\Psi)}{4\pi}$ |
|---|---|---|---|
| 1 | 7.563 | 7.559 | 7.434 |
| 2 | 5.395 | 5.391 | 5.570 |
| 3 | 3.531 | 3.563 | 3.678 |
| 5 | 1.923 | 1.939 | 1.771 |
| 7 | 1.317 | 1.330 | 1.366 |
| 10 | 0.898 | 0.935 | 1.084 |
| 15 | 0.642 | 0.631 | 0.658 |
| 20 | 0.426 | 0.456 | 0.377 |

TABLE 3. Parameters characterizing derived Gaussian approximations: $\alpha$–$\delta$ in units of radians$^2$.

| | $\frac{1}{4\pi}\hat{\mathcal{P}}_a^{(8)}(\Psi)$ | | |
|---|---|---|---|
| $A$ | 4.965 | $\alpha$ | 1.480 E-3 |
| $B$ | 2.225 | $\beta$ | 6.282 E-3 |
| $C$ | 0.790 | $\gamma$ | 3.840 E-2 |
| $D$ | 0.615 | $\delta$ | 3.264 E-1 |
| | $\frac{1}{4\pi}\hat{\mathcal{P}}_a^{(4)}(\Psi)$ | | |
| $A$ | 6.539 | $\alpha$ | 2.369 E-3 |
| $B$ | 1.442 | $\beta$ | 5.701 E-2 |
| $C$ | 0.250* | $\gamma$ | 6.500 E-1 |

* Predetermined.

[2] This analytical approximation was found to be valid for $\tau_m=0.001$, $\tau_a=2.0$, the phase function presented in Table 1, and $\mu=\mu_0=\cos 70°$, provided that $\phi\lesssim 35°$.

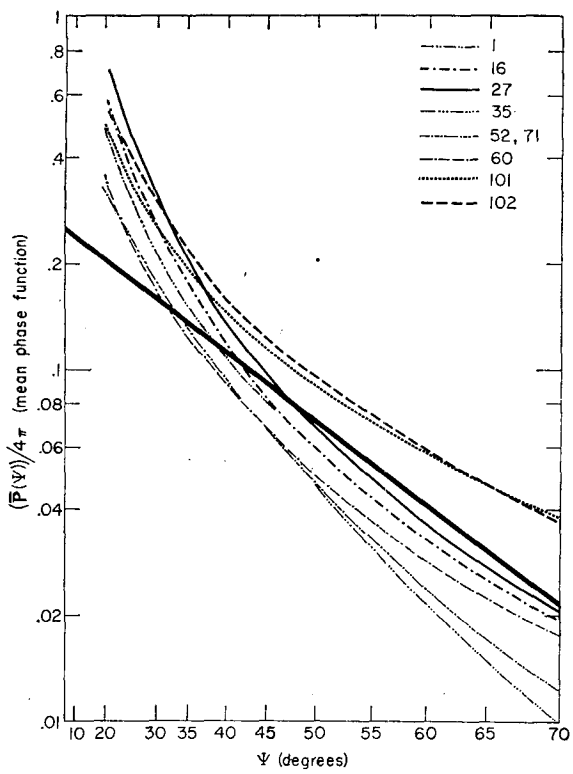


FIG. 2. Mean phase functions computed by Deirmendjian (1969). Numbers designate tables in Deirmendjian's monograph. Solid line defines $C$ and $\gamma$ used in $[\hat{\bar{\mathcal{P}}}_a^{(4)}(\Psi)]/4\pi$.

characterized by the quantity

$$\frac{\left\{\sum_{i=1}^{I}\left[\log\left(\frac{\hat{\bar{\mathcal{P}}}_a(\Psi_i)}{4\pi}\right)-\log\left(\frac{\bar{\bar{\mathcal{P}}}_a(\Psi_i)}{4\pi}\right)\right]^2\right\}^{\frac{1}{2}}}{\sum_{i=1}^{I}\log\left(\frac{\hat{\bar{\mathcal{P}}}_a(\Psi_i)}{4\pi}\right)}. \quad (18)$$

If only eight simulated noise free measurements are available, then a Gaussian approximation with less than eight parameters is feasible. A six-parameter Gaussian approximation was therefore fitted to an equation of the form of (17). Of the six parameters,

TABLE 4a. Effect of 3% random noise in simulated aureole measurements on the approximate phase function $[\hat{\bar{\mathcal{P}}}_a^{(8)}(\Psi)]/4\pi$.

| Ψ (deg) | Trial 1 | Trial 2 | Trial 3 | Trial 4 |
|---|---|---|---|---|
| 1 | 7.419 | 7.690 | 7.602 | 7.610 |
| 2 | 5.369 | 5.346 | 5.410 | 5.466 |
| 3 | 3.601 | 3.548 | 3.624 | 3.589 |
| 5 | 1.887 | 1.881 | 2.013 | 1.894 |
| 7 | 1.283 | 1.260 | 1.340 | 1.307 |
| 10 | 0.916 | 0.920 | 0.941 | 0.925 |
| 15 | 0.611 | 0.588 | 0.670 | 0.612 |
| 20 | 0.472 | 0.409 | 0.456 | 0.431 |

TABLE 4b. Parameters characterizing phase functions derived from noisy data: $\alpha$–$\delta$ in units of radians$^2$.

| | | | | |
|---|---|---|---|---|
| $A$ | 3.608 | 3.976 | 4.747 | 5.178 |
| $B$ | 3.065 | 3.436 | 2.737 | 2.046 |
| $C$ | 1.038 | 1.055 | 0.690 | 0.893 |
| $D$ | 0.687 | 0.432 | 0.499 | 0.492 |
| $\alpha$ | 1.330 E-3 | 1.098 E-3 | 1.369 E-3 | 1.601 E-3 |
| $\beta$ | 3.965 E-3 | 4.251 E-2 | 6.743 E-3 | 6.323 E-3 |
| $\gamma$ | 2.396 E-2 | 4.156 E-2 | 7.800* E-2 | 4.436 E-2 |
| $\delta$ | 3.126 E-1 | 6.000* E-1 | 2.591 E-1 | 4.452 E-1 |

* Predetermined limit on the range of parameter values.

only four were optimized and the remaining two, $C$ and $\gamma$, were predetermined. These latter parameters do not have to be known with great accuracy because they describe scattering at angles $>30°$. The significance of that scattering is relatively minor although it is not negligible if $\Psi \lesssim 5.2°$ ($\phi \lesssim 20°$).

The parameters which characterize the approximate phase function at large scattering angles were obtained by graphically approximating a Gaussian function to the mean of several phase functions computed by Deirmendjian (1969). Fig. 2 shows phase functions for aerosols characterized by several size distributions and refractive indices; these are plotted as $\log[\bar{\mathcal{P}}_a(\Psi)]/4\pi$ vs $\Psi^2$. The numbers refer to the table designation in Deirmendjian's monograph. The bold line represents a Gaussian characterized by the values of $C$ and $\gamma$ which were employed in the derivation of $[\hat{\bar{\mathcal{P}}}_a^{(4)}(\Psi)]/4\pi$.

Table 3 shows that $[\hat{\bar{\mathcal{P}}}_a^{(4)}(\Psi)]/4\pi$ agrees with $[\bar{\mathcal{P}}_a(\Psi)]/4\pi$ within 5.5%. These results are poorer than the previous case because the number of measurements

TABLE 5a. Effect of 10% random noise in simulated aureole measurements on the approximate phase functions $[\hat{\bar{\mathcal{P}}}_a^{(8)}(\Psi)]/4\pi$.

| Ψ (deg) | Trial 1 | Trial 2 | Trial 3 | Trial 4 |
|---|---|---|---|---|
| 1 | 7.316 | 7.480 | 7.362 | 7.571 |
| 2 | 5.149 | 5.382 | 5.280 | 5.790 |
| 3 | 3.476 | 3.515 | 3.484 | 3.999 |
| 5 | 1.852 | 1.835 | 1.899 | 2.070 |
| 7 | 1.269 | 1.291 | 1.312 | 1.393 |
| 10 | 0.954 | 0.922 | 0.903 | 0.905 |
| 15 | 0.620 | 0.614 | 0.619 | 0.608 |
| 20 | 0.424 | 0.439 | 0.422 | 0.451 |

TABLE 5b. Parameters characterizing phase functions derived from noisy data: $\alpha$–$\delta$ in units of radians$^2$.

| | | | | |
|---|---|---|---|---|
| $A$ | 3.279 | 5.318 | 5.163 | 5.398 |
| $B$ | 3.653 | 1.697 | 2.036 | 1.961 |
| $C$ | 0.979 | 0.786 | 0.731 | 0.547 |
| $D$ | 0.533 | 0.645 | 0.410 | 0.433 |
| $\alpha$ | 1.024 E-3 | 1.682 E-3 | 1.591 E-3 | 2.148 E-3 |
| $\beta$ | 3.895 E-3 | 6.414 E-3 | 8.113 E-3 | 1.117 E-2 |
| $\gamma$ | 4.087 E-2 | 3.499 E-2 | 7.258 E-2 | 7.800* E-2 |
| $\delta$ | 3.466 E-1 | 2.748 E-1 | 3.578 E-1 | 4.819 E-1 |

* Predetermined limit on the range of parameter values.

and the number of adjustable parameters in the approximate phase function have been reduced.

The effect of noise in the simulated measurements on the phase functions derived from these measurements is presented in Tables 4–6. Three different combinations of random noise are presented in each case to illustrate the magnitude of variations in the derived phase functions. Although the output of the cases considered in Tables 4 and 5 produced phase function data at 20 angles, the presentation is restricted to 8 angles for conciseness.

The inverted phase functions $[\hat{\mathcal{P}}_a^{(8)}(\Psi)]/4\pi$ shown in Table 4 agree with the actual phase function $[\bar{\mathcal{P}}_a(\Psi)]/4\pi$ within about 2% when the multiply scattered intensities at 20 angles have a 3% random noise superimposed. The phase functions $[\hat{\mathcal{P}}_a^{(8)}(\Psi)]/4\pi$ shown in Table 5 agree with the actual phase function $[\bar{\mathcal{P}}_a(\Psi)]/4\pi$ within about 8% when the multiply scattered intensities at 20 angles have a 10% random noise superimposed. These examples demonstrate that an approximate Gaussian phase function with eight adjustable parameters is the best that any set of 20 measurements is likely to yield. In fact, the Gaussians average the noisy data over limited angular ranges so that they seem to reduce the deviation of the inverted phase function to a value which is slightly less than the noise in the input data.

Table 3 shows that $[\hat{\mathcal{P}}_a^{(4)}(\Psi)]/4\pi$ could only come within 5.5% of $[\bar{\mathcal{P}}_a(\Psi)]/4\pi$ when the measured intensity is noiseless. Subsequent studies showed that the direct application of this approximation would only be useful if the noise in the measured intensity exceeded 6%.

Table 6 shows the approximate phase functions $[\hat{\mathcal{P}}_a^{(4)}(\Psi)]/4\pi$ inverted from intensities with 10% noise measured at 8 angles. The inverted phase functions are within 10% of $[\bar{\mathcal{P}}_a(\Psi)]/4\pi$.

One strategy to improve the accuracy of the phase function derived from noisy aureole measurements taken at 8 angles is to use $[\hat{\mathcal{P}}_a^{(4)}(\Psi)]/4\pi$ to account for multiply scattered intensities [terms with $n \geqslant 2$ in Eq. (17)]. Subtracting the multiply scattered intensity from the measured intensity yields the singly scattered intensity which is proportional to the phase function.

The following paper by Twitty will show how particle size distributions can be inverted from phase functions.

## 6. Conclusion

A small-angle approximation to the solution of the equation of radiative transfer is derived. It is shown that if the phase function which represents a single scattering event is sufficiently anisotropic, and if the optical depth is modest, then the computed approximate intensity is within a few percent of the intensity computed by rigorous numerical methods.

A series of Gaussian functions is employed to approximate the phase function at small scattering angles. If the number of Gaussian terms is about one-fourth of the number of measurements, then the constants in the Gaussian terms can be obtained from those measurements by an optimizing procedure. Noise in the measurements is transformed into noise of comparable magnitude in the inferred approximate phase function.

TABLE 6a. Effect of 10% random noise in simulated aureole measurements on the approximate phase function $[\hat{\mathcal{P}}_a^{(4)}(\Psi)]/4\pi$.

| $\Psi$ (deg) | Trial 1 | Trial 2 | Trial 3 | Trial 4 |
|---|---|---|---|---|
| 1 | 7.510 | 7.974 | 7.425 | 8.686 |
| 2 | 5.590 | 5.827 | 5.714 | 5.964 |
| 3 | 3.616 | 3.714 | 3.927 | 3.502 |
| 5 | 1.589 | 1.725 | 1.997 | 1.559 |
| 7 | 1.191 | 1.355 | 1.509 | 1.278 |
| 10 | 0.985 | 1.099 | 1.139 | 1.051 |
| 15 | 0.659 | 0.694 | 0.629 | 0.679 |
| 20 | 0.411 | 0.408 | 0.339 | 0.408 |

TABLE 6b. Parameters characterizing phase functions derived from noisy data: $\alpha$–$\gamma$ in units of radians$^2$.

| | | | | |
|---|---|---|---|---|
| $A$ | 6.924 | 7.259 | 6.187 | 8.375 |
| $B$ | 1.151 | 1.398 | 1.710 | 1.294 |
| $C$ | 0.250 | 0.250 | 0.250 | 0.250 |
| $\alpha$ | 2.448 E-3 | 2.234 E-3 | 2.497 E-3 | 1.923 E-3 |
| $\beta$ | 7.030 E-2 | 6.277 E-2 | 4.753 E-2 | 6.541 E-2 |
| $\gamma$ | 6.500 E-1 | 6.500 E-1 | 6.500 E-1 | 6.500 E-1 |

*Acknowledgments.* We wish to thank Mr. Peter Guetter, University of Wisconsin, for his efforts in programming the computations employed in this study.

Funds were provided from grants NASA-50-002-140 and NASA NGR 03-002-155. We wish to thank NASA for its support of this work.

## REFERENCES

Dave, J. V., 1968: Subroutines for computing the parameter of the electromagnetic radiation scattered by a sphere. I.B.M. Tech. Rept. 320, 3237.

Deirmendjian, D., 1969: *Electromagnetic scattering on Spherical Polydispersions.* Elsevier, 290 pp.

——, 1971: Global turbidity studies I, Volcanic dust effects—a critical survey. Rand document R886-ARPA, 31 pp.

Herman, B. M., and S. R. Browning, 1965: A numerical solution to the equation of radiative transfer. *J. Atmos. Sci.* **22**, 559–566.

Irvine, W. M., 1965: Multiple scattering by large particles. *Astrophys. J.*, **142**, 1563–1575.

Junge, C. E., 1963: *Air Chemistry and Radioactivity.* Academic Press, 382 pp.

Marquardt, D. L., 1963: An algorithm for least squares estimation of non-linear parameters. SIAM *J. Appl. Math.*, **2**, 431–441.

Sneddon, I. H., 1972: *The Use of Integral Transforms.* McGraw-Hill, 539 pp.

Twitty, J. T., 1975: Inversion of aurole measurements to derive aerosol size distributions, *J. Atmos. Sci.*, **32**, 584–591.

Weinman, J. A., 1968: Axially symmetric transfer of light through a cloud of anisotropically scattering particles. *Icarus* **9**, 67–73.